Curr Treat Options Cardio Med (2019) 21:55
DOI 10.1007/s11936-019-0756-x

Imaging (Q Truong, Section Editor)

Multimodality Imaging in the Evaluation of Intracardiac Masses

Carolyn M. Wu, MD, MS[1]
Peter J. Bergquist, MD[2]
Monvadi B. Srichai, MD[1,2,*]

Address
[*,1]Department of Cardiology, MedStar Georgetown University Hospital, MedStar Washington Hospital Center, MedStar Heart and Vascular Institute, Washington, DC, 20007, USA
Email: srichai@alum.mit.edu
[2]Department of Radiology & Department of Radiology, Medstar Georgetown University Hospital, 3800 Reservoir Road NW, 5PHC, Washington, DC, 20007, USA

This article is part of the Topical Collection on *Imaging*

Keywords Intracardiac masses · Multimodality imaging · Cardiac MRI · Cardiac CT · Echocardiography · Positron emission tomography

Abstract

Intracardiac masses are classified as neoplastic or non-neoplastic. Prognosis varies based on the diagnosis of the mass since treatment options differ greatly. As novel imaging techniques emerge, a multimodality approach to the evaluation of intracardiac masses becomes an important part of non-invasive evaluation prior to potential surgical planning or oncological treatment. The purpose of this article is to compare the available imaging modalities—echocardiography, cardiovascular magnetic resonance, cardiac computed tomography, nuclear imaging, and emerging novel hybrid imaging techniques for future clinical applications—and to review the characteristic features seen on those modalities for the most common intracardiac masses.

Introduction

Cardiac masses are commonly classified as neoplastic (primary and secondary) or non-neoplastic (e.g., thrombus or vegetation). Cardiac tumors are rare, with an estimated autopsy prevalence of < 0.1% for primary tumor and about 1.2% for secondary tumors [1]. Cardiac thrombi are more common, with a prevalence up to 25% and 50% in patients with atrial fibrillation and left ventricular systolic dysfunction, respectively [2], as well as misinterpreted normal anatomical variants [3]. Differentiating between these masses is paramount

Published online: 05 September 2019

as treatment options differ greatly. A classification scheme of intracardiac masses is shown in Table 1, based on the 2015 World Health Organization's classification of tumors of the heart [4]. This review discusses the complementary nature of multimodality imaging assessment and surveillance of intracardiac masses.

Imaging modalities

Echocardiography

Transthoracic echocardiography (TTE) is considered the first-line imaging modality for the assessment of cardiac masses due to its portability, lack of radiation, and wide availability. It remains the most often used modality to characterize masses and their hemodynamic consequences, as many masses are found incidentally with echocardiography [5]. With its high temporal and spatial resolution, echocardiography remains the best modality for evaluating valvular lesions or small highly mobile masses, particularly in the setting of arrhythmias or frequent ectopy. TTE has sensitivity 55–93% of detecting intracardiac masses [6].

Transesophageal echocardiography (TEE) is used to complement TTE with improved detection of cardiac masses compared to TTE alone, particularly in the evaluation of posterior structures and small lesions [6]. It increases detection of left atrial thrombi, right atrial, and extracardiac lesions [7].

Newer techniques in echocardiography have slowly gained utility in the evaluation of intracardiac masses. The use of microbubble contrast agents can confirm the presence of a cardiac mass and provide information on perfusion, a marker of vascularity [8••,9]. 3D images are increasingly used for better volumetric assessment of masses [10,11] and strain imaging for distinguishing between masses based on tissue deformation properties [12,13].

The major advantage of echocardiography is that it allows for follow-up imaging over time without extra exposure to radiation. Despite its wide availability, echocardiography has known limitations including operator dependence, potential poor acoustic windows, and artifacts that can sometimes be misinterpreted as masses [13•,14].

Cardiovascular magnetic resonance

Cardiovascular magnetic resonance (CMR) offers multiplanar assessment of cardiac masses, with high spatial resolution and unrestricted field of view without exposure to radiation [14,15]. It is used for more definitive characterization of a mass following the initial detection by other imaging modalities. CMR provides information on mass size, shape, location, attachment, and secondary anatomic and hemodynamic effects on ventricular and valvular function.

The main strength of CMR is its ability to provide unique information on tissue composition of the mass based on proton density and intrinsic relaxation parameters such as T1, T2, and T2 star values using T1- and T2-weighted and/or parametric mapping sequences [16]. Evaluation of contrast uptake kinetics with first-pass perfusion and late gadolinium enhancement (LGE) sequences can be applied for further insight into tissue characteristics. LGE imaging using prolonged inversion time can further distinguish tumors from thrombi, with any enhancement within the mass as more suggestive of a tumor. CMR has been proven to improve detection of cardiac masses which may not be visualized on routine TTE [17] and provides a high accuracy for discriminating between

Table 1. World Health Organization 2015 classification of tumors of the heart and common non-neoplastic cardiac masses

Benign tumors and tumor-like conditions
Rhabdomyoma
Histiocytoid cardiomyopathy
Hamartoma of mature cardiac myocytes
Adult cellular rhabdomyoma
Cardiac myxoma
Papillary fibroelastoma
Hemangioma (capillary, cavernous, arteriovenous malformation, intramuscular)
Cardiac fibroma
Lipoma
Cystic tumor of the atrioventricular node
Granular cell tumor
Schwannoma
Tumors of uncertain biologic behavior
Inflammatory myofibroblastic tumor
Paraganglioma
Germ cell tumors
Teratoma (mature, immature)
Yolk sac tumor
Malignant tumors
Angiosarcoma
Undifferentiated pleomorphic sarcoma
Osteosarcoma
Myxofibrosarcoma
Leiomyosarcoma
Rhabdomyosarcoma
Synovial sarcoma
Miscellaneous sarcomas
Cardiac lymphomas
Metastatic tumors
Non-neoplastic
Thrombus
Vegetation
Coumadin ridge
Crista terminalis
Caseous mitral annulus calcification

benign and malignant lesions with high interobserver agreement [18]. CMR may also provide additional information on the resectability of masses and

associated complications such as invasion into adjacent mediastinal structures, regional or distant metastases, and encasement of vital structures. In addition to cine steady-state free precession (SSFP) imaging, radiofrequency tissue tagging sequences can be help delineate intramyocardial tumors, particularly for determining whether there is myocardial infiltration, pericardial involvement, or a dissection plane that renders the tumor potentially operable. CMR imaging protocols incorporate multiple different pulse sequences described above, commonly in multiple imaging planes.

The primary limitation of CMR is the lack of availability and expertise in most centers to perform and interpret these studies. Additionally, patients may not tolerate the examination due to claustrophobia or difficulty remaining still with repetitive breath holding during imaging acquisition. They could also have contraindications related to metallic implants (e.g., non-conditional pacemakers), pregnancy, and/or relative contraindications to the use of gadolinium contrast (e.g., renal failure).

Cardiac computed tomography

Cardiac computed tomography (CCT) is considered an appropriate test for the initial and follow-up evaluation of cardiac masses [19••] and often complements the information provided by echocardiography or CMR. In particular, CCT is frequently considered when other modalities are not feasible or if images are equivocal with those modalities [20]. Cardiac masses may also be incidentally identified on chest computed tomography (CT) studies performed for other reasons. As with CMR, CCT can provide information on mass size, shape, location, attachment, invasion into the myocardium and, depending on the imaging protocol, secondary anatomic effects on ventricular and valvular function. CCT provides some limited tissue characterization and is particularly sensitive for detection of calcium and fat. Delayed imaging can further characterize masses, particularly if thrombus is suspected in a region with slow flow. Compared to other techniques, CCT has the advantage to detect calcifications within a mass and delineate the coronary artery anatomy, which helps distinguish mass-like vascular lesions such as coronary artery or bypass graft aneurysms from true cardiac masses.

Dual-energy CT (DECT) is a relatively new CT imaging technique which can provide additional information in evaluating cardiac masses. By acquiring two simultaneous datasets with different photon energy spectra, tissue characteristics can be extracted from the images. DECT is sensitive to the presence of iodine within a tissue due to the unique interactions of iodine with X-rays of differing energies. Iodine concentrations can be quantitatively calculated within a region of interest. This technique has been applied to distinguish cardiac tumors from thrombus more reliably on CT. Cardiac tumors may have similar Hounsfield units to thrombus on CT; the subtle differences in iodine concentration can be detected with DECT [21,22]. CMR still performs better than DECT in distinguishing tumors from thrombi, but for a patient unable to undergo CMR, DECT can be a useful alternative. Beyond this, there is the potential for quantitative iodine values of an unknown cardiac mass to aim diagnosis once more data become available regarding DECT of different known cardiac tumors.

The main limitations of CCT are radiation exposure, which has significantly decreased recently with dose reduction protocols, risk of

contrast-induced nephropathy, and lower soft tissue and temporal resolutions as compared with CMR.

Nuclear imaging

Due to its disadvantages with high radiation and limited spatial resolution, nuclear imaging for cardiac masses is not generally used except in certain scenarios. In evaluation of cardiac carcinoid tumors, octreotide single-photon emission computed tomography (SPECT) is often useful, while positron emission tomography (PET) with ^{18}F-fluorodexyglucose (^{18}F-FDG) is useful for staging, restaging, or evaluating response to therapy of systemic malignancies that may involve the heart [14]. A 24-h dietary restriction with a high-fat and low-carbohydrate diet is often required prior to PET imaging in order to shift myocardial metabolism to achieve adequate evaluation of an intracardiac lesion [23]. Based on the mean of the maximal standardized uptake value (SUV_{max}), benign cardiac tumors can be differentiated from malignant primary or secondary cardiac tumors, which tend to have higher SUV_{max} [24,25]. When interpreting studies using ^{18}F-FDG PET, one needs to be cautious with false positive findings such as lipomatous hypertrophy that frequently shows mild ^{18}F-FDG update from brown fat activation [26] and avid inflammatory or infectious lesions that could mimic malignant tumors. ^{18}F-FDG PET allows for determination of malignant potential of doubtful masses, assessment of disease stage including myocardial involvement and pericardial spread, and evaluation of postoperative residual disease and response to chemotherapy [23].

Hybrid imaging

Hybrid imaging refers to software or hardware image fusion techniques that allow intrinsic combination of image information from at least two different modalities. Hybrid imaging, particularly when combined with PET imaging, plays a central role in the diagnosis and management of malignancies, including cardiac tumors [27]. Initial work on hybrid imaging focused on software techniques with fusion of different imaging datasets, allowing for display of anatomic and functional information together. With the rapid development of innovative techniques, novel hybrid, multimodality imaging systems have also emerged, including the use of PET/CT and PET/MRI systems, which have been used to improve evaluation of cardiac masses.

Whole-body ^{18}F-FDG PET/CT takes advantage of the combined metabolic-morphologic properties of PET and CT, respectively [24]. It is recommended for evaluating potential underlying malignancy in patients with suspected metastatic malignant tumors to the heart on echocardiography or CMR, providing disease staging, and evaluating postoperative residual disease and response to chemotherapy [23]. Integrated ^{18}F-FDG PET/MRI is another novel imaging technique in development that utilizes the advantage of PET and MRI in a single study [25,28]. This combination allows morphological tissue characterization with MRI and information about tumor metabolism with PET for cardiac tumor evaluation [28]. Hybrid ultrasound-MRI systems are in development and have been shown to improve cardiac imaging through real-time tracking of organ position via the integrated ultrasound system [29]. The true benefits of these hybrid technologies are still under investigation, particularly given the potential associated costs and limited availability of these technologists, but may include

information such as planning of surgical procedures in complex cases and/or differentiation of scar tissue versus relapse in follow-up imaging after surgery, radiation, or chemotherapy treatment [30].

Diagnostic evaluation of cardiac masses

Depending on clinical scenario, the use of multiple imaging modalities may be important for optimal management of a patient's condition. Patients often undergo TTE for initial evaluation of suspected cardiac disease. As such, TTE is usually the first imaging modality in the evaluation of cardiac masses including incidentally noted lesions. Patients with small, highly mobile lesions, valvular masses or posteriorly located lesions, are often referred for TEE to better delineate and characterize these lesions, particularly when vegetation is suspected. With other masses, it may be appropriate to refer the patient for further imaging to confirm and/or provide additional information on diagnosis, extent of involvement, and treatment planning. The next imaging test depends on the initial imaging finding, availability of imaging modalities, institution expertise, and clinical situation. If diagnosis is clear from TTE and clinical situation, then no further imaging is needed. However, when diagnosis is unclear, CMR is the next best step as CMR provides the most comprehensive tissue characterization compared to other modalities, particularly distinguishing between benign and malignant lesions. CCT may be useful in patients who cannot undergo CMR or who have non-diagnostic CMR. Similarly, for patients with incidentally noted cardiac masses on chest CT, X-ray, or nuclear cardiac imaging, CMR or TTE may better define the lesion including functional, anatomic, and hemodynamic consequences on ventricular or valvular function. For specific tumors under consideration such as carcinoid tumors, octreotide SPECT may be important for non-invasive diagnosis and management. Finally, for lesions with unclear diagnosis using the above modalities, FDG PET may provide additional information on the metabolic activity within lesions to help in the differentiation.

Figure 1 shows the proposed general approach to choosing an imaging modality in evaluating intracardiac masses. Table 2 shows the characteristic features of common intracardiac masses seen on echocardiography, CMR, and CCT [14,31,32].

Intracardiac thrombus

Intracardiac thrombi are one of the most common cardiac masses, often seen in the left atrial appendage (LAA) associated with atrial fibrillation or mitral valvular disease, or in areas of akinesis or ventricular aneurysms, and as a thrombus-in-transit from venous thromboembolism in the right ventricle [33]. On TTE, acute thrombi appear rounded with smooth contours, while chronic thrombi can appear as linear or crescentic lesions along the endocardial surface. On CMR, acute/subacute thrombi demonstrate increased T1 and T2 depending on age, whereas chronic thrombi have low T1 and T2 signal. With first-pass perfusion and LGE, most thrombi remain hypointense for both sequences [2]. On CCT, thrombi appear as low attenuation, non-enhancing lesions on post-contrast images. The use of delayed CT imaging improves the specificity for detection of thrombus. This is particular useful in detection of LAA thrombi

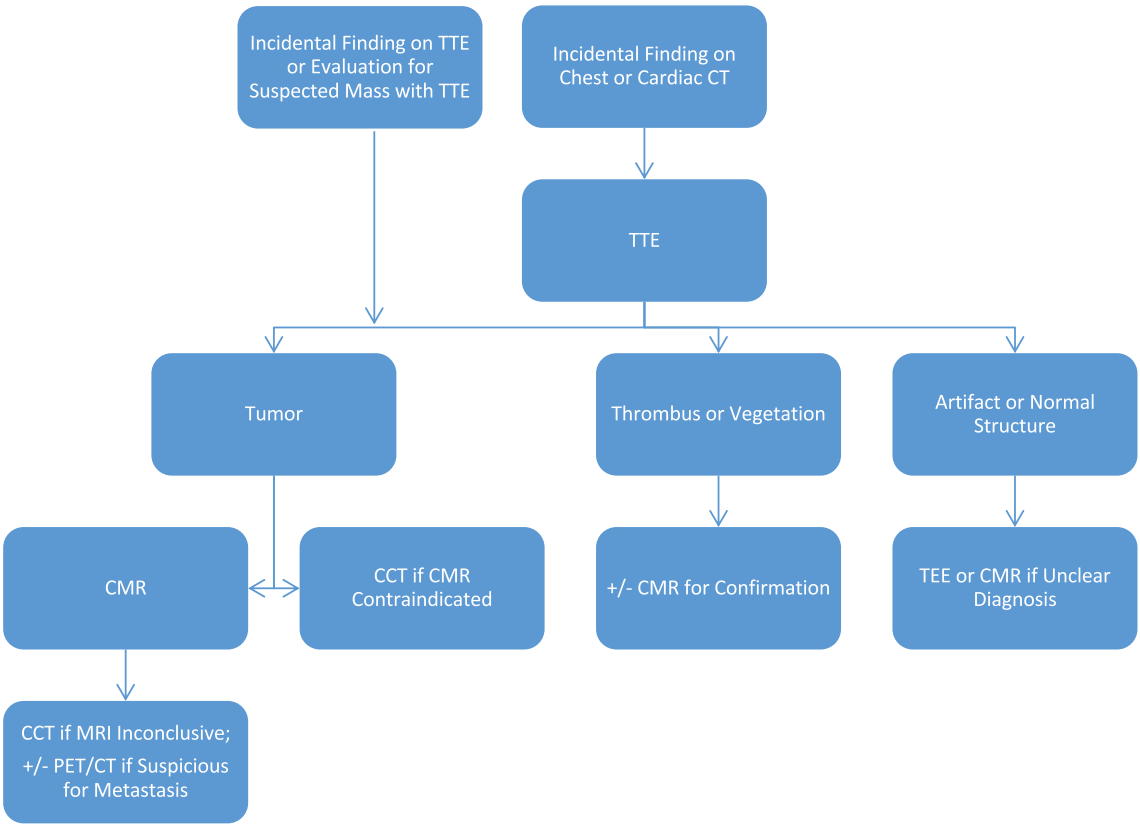

Fig. 1. Proposed general algorithm in multimodality evaluating intracardiac masses. *TTE* transthoracic echocardiography, *CT* computed tomography, *CMR* cardiovascular magnetic resonance, *CCT* cardiac computed tomography, *PET* positron emission tomography, *TEE* transesophageal echocardiography.

where stasis of blood can simulate a thrombus on early arterial images [34]. PET imaging of thrombus demonstrates no uptake of ^{18}F-FDG.

Normal intracardiac and tumor-like structures

Normal intracardiac structures such as the Coumadin ridge, Eustachian valve, Chiari network, and crista terminalis can sometimes be mistaken for tumors or thrombi on TTE [3,14]. Those structures generally can be easily distinguished with CMR or CCT. Interatrial septal aneurysm can often be misinterpreted as a cystic intracardiac mass, and lipomatous hypertrophy can be misinterpreted as a myxoma or fibroma on TTE [13•]. Caseous calcification of mitral annulus can sometimes be mistaken for a tumor on echocardiogram, but can be better evaluated on CT for its characteristic calcified wall to suggest the correct diagnosis [35].

Benign primary tumors

Cardiac myxoma

Cardiac myxomas are the most common primary benign cardiac tumors, about 50–80% of cases [36]. The majority are found in the left atrium,

Table 2. Characteristic finding of common cardiac masses on different imaging modalities

Intracardiac masses	Echocardiography	CMR	CCT	Characteristics; common locations
Cardiac myxoma	Hyperechogenic	T1: hypo/isointense; T2: hyperintense; fat saturation: no change; LGE: high, heterogeneous	Hypodense; calcifications; high iodine concentration on DECT	Lobular; intracavitary, LA (75%), RA (20%), ventricles (5%)
Papillary fibroelastoma	Heterogeneous	T1/T2: hyperintense, homogeneous; LGE: high, homogeneous delayed	Hypodense	Frond, pedicle; valvular
Rhabdomyoma	Hyperechogenic; opposite deformation from myocardium	T1: isointense; T2: iso/hyperintense; LGE: no/minimal	Hypodense	Smooth, broad base; intramural
Fibroma	Hyperechogenic; no deformation on strain	T1: isointense; T2: hypointense; LGE: hyperenhance	Hypodense; punctate calcification enhancement	Smooth, broad base; intramural
Lipoma	Homogeneous, hyperechogenic	T1/T2: hyperintense; fat saturation: hypointense; LGE: no/minimal	Hypodense; fat attenuation	Smooth, broad base; interatrial septum, intramural, intracavitary
Hemangioma	Enhancement with contrast	T1: isointense, heterogeneous; T2: hyperintense; first-pass: strong LGE: absent	Hypodense; punctate calcifications intense enhancement	Intracavitary
Sarcomas	Isoechogenic to hyperechogenic	T1: iso (rhabdo-,undif.)/ heterogeneous (angio-); T2: heterogeneous (angio-)/ hyperintense (rhabdo-, undif.); LGE: heterogeneous (angio-), homogeneous (rhabdo-)	Isodense	Lobular; broad base; LA (undifferentiated, osteo-, fibro-, leiomyosarcoma), RA (angiosarcoma), LV (rhabdomyosarcoma)
Lymphoma	Homogeneous echogenicity, thickened wall	T1: isointense, homogeneous; T2: isointense; LGE: minimal	Hypo/isodense	Lobular; RA, RV, mediastinum
Metastatic tumor	Iso/hyperechogenic	T1: hypo/isointense; T2: iso/hyperintense; LGE: heterogeneous, strong	Isodense; +/– calcifications	Multiple locations
Thrombus	Hyperechogenic	T1: homogenous, high (low if chronic); T2: iso/high (low if chronic); fat saturation: isointense; first-pass perfusion and LGE: hypointense	Low attenuation, non-enhancing; crescentic shape (chronic)	LAA, apical thrombus with severe LV systolic dysfunction

CMR cardiovascular magnetic resonance, *CCT* cardiac computed tomography, *LGE* late gadolinium enhancement, *DECT* dual-energy computed tomography, *LA* left atrium, *RA* right atrium, *LV* left ventricle, *RV* right ventricle, *LAA* left atrial appendage

originating from the interatrial septum [37]. Prior to cardiac ultrasound, coronary angiography was the only method to detect the presence of the tumor with its neovascularization [38]. TTE can define the location, size, attachment, mobility of the mass, hemodynamic effects [36], and vascularity by color Doppler [39]. When TTE is suboptimal, TEE may be considered to improve acoustic field of view, and is superior to TTE in identification of attachment point, especially for right atrial myxomas [40]. Echo contrast perfusion and 3D imaging can also be helpful for further characterization of cardiac myxoma. After surgical resection, recurrence surveillance with follow-up echocardiogram is recommended for familial cases [37].

On CMR, myxomas often have a characteristic pattern, the "blackberry" appearance, with areas of isointensity on T1, hyper-intensity on T2 due to high extracellular water content, and foci of hypointensity on both T1 and T2 images representing regions of acute hemorrhage. On SSFP, myxomas appear hyperintense relative to myocardium but hypointense relative to blood [13,36,41]. Another pattern seen less frequently is one with low signal intensity on T1, T2, and cine imaging, mimicking a thrombus [36]. A third pattern is a homogenous hyperintensity at T2 imaging with a "pseudocystic" appearance [36]. As myxomas may contain cysts, regions of necrosis, fibrosis, hemorrhage, and calcification, post-contrast images typically demonstrate heterogeneous enhancement. Additionally, many myxomas have surface thrombus which demonstrate low signal intensity on LGE images [42].

In most cases, CCT attenuation of myxomas on both pre-contrast and post-contrast images has only limited ability to differentiate myxomas from thrombi, and therefore, CT is not frequently used as the modality for further characterization of suspected myxomas [36]. However, DECT can more easily distinguish myxoma from thrombi with the presence of higher measured iodine concentration [22].

^{18}F-FDG PET evaluation of myxomas remains limited, showing no or low ^{18}F-FDG uptake [43].

Papillary fibroelastoma

Papillary fibroelastomas, the third most prevalent benign cardiac tumor [44], can arise from any endocardial surface but most commonly noted on the upstream side of cardiac valves with aortic valve being most often involved [45]. Their "frond-like" appearance can be easily visualized as a small pedunculated mass on TTE. TEE is more sensitive in detecting papillary fibroelastomas, especially when they are small, reinforcing its role in the evaluation of embolic strokes [8]. On CMR, they typically appear as a well-defined small homogeneous valvular mass that appears hypointense on SSFP and homogenous on LGE imaging. On CCT, papillary fibroelastomas appear hypodense with irregular borders attached by a thin stalk but may be difficult to visualize due to their small size.

Rhabdomyoma

Rhabdomyomas, the most common benign cardiac tumors in children but rare in adulthood, are associated with tuberous sclerosis and tend to be multiple [13,46]. They appear more echogenic than the surrounding myocardium within ventricular walls or on atrioventricular valves [8,46]. Echocardiographic deformation imaging has been used for rhabdomyomas, which shows the deformation in the opposite direction of the myocardium, suggesting elasticity in the tumor cells [12]. Rhabdomyomas appear isointense to myocardium on T1-weighted images and iso- to hyperintense on T2-weighted images with variable enhancement pattern [32,47]. Tissue tagging sequences can delineate tissue planes between tumor and myocardium as well as demonstrate deformation of the tumor due to compression by the myocardium. On CCT, rhabdomyomas demonstrate smooth borders with attenuation similar to myocardium. The lack of calcifications helps distinguish rhabdomyoma from fibromas. In the presence of small intramyocardial lesions, echocardiography and CCT may only demonstrate diffuse myocardial thickening whereas contrast-enhanced CMR can better define the borders of these tumors [48].

Fibroma

Cardiac fibromas, the second most common benign cardiac tumors in infants and children, associated with Gorlin syndrome, often show punctate calcifications within large, intramural masses [13,49], which can be readily detected by CCT, distinguishing it from other cardiac tumors seen in this age group such as rhabdomyoma. On TTE, fibromas appear well-demarcated, non-contractile, highly echogenic, frequently located in the ventricular free wall, anterior, or septal walls [8]. They do not show any deformation comparing to myocardium due to its non-compliant composition of fibrotic tissues [12]. On CMR, fibromas are isointense relative to normal myocardium on T1 images and hypointense on T2 images with homogenous appearance unless there are central calcifications, which may be seen as patchy areas of hypointensity within the tumor. Fibromas generally show no contrast enhancement on first-pass perfusion with intense hyperenhancement noted on LGE images. Tissue tagging sequences further delineate borders of the tumor which is non-deforming compared to the surrounding myocardium.

Lipoma

Lipomas are often seen in the pericardial space but can appear as intracardiac masses, arising from the subendocardium or on the valves [13]. On TTE, they appear immobile, well circumscribed, homogenous, and broad based without a pedicle [8]. The key diagnostic finding on CMR is homogeneous high signal intensity on T1-weighted images that markedly suppress with the application of fat-saturation pulses. Additionally, lipomas generally do not enhance with application of contrast material [42]. Fat attenuation on CCT can help differentiating them as cardiac lipomas.

Hemangiomas

Various types of hemangiomas exist, including capillary hemangiomas, cavernous hemangiomas, arteriovenous malformation, and intramuscular hemangiomas [4]. They are benign vascular tumors that can be found anywhere in the heart or in the pericardium [50]. However due to the presence of various types of hemangiomas, no typical echocardiographic tissue characteristics can be used to distinguish this tumor as a whole. The use of contrast echocardiography may allow further characterization of hemangiomas by demonstrating the vascularity of the lesion which demonstrates high and rapid contrast enhancement compared to the adjacent myocardium [51]. CCT and CMR provide additional information on the invasiveness of the tumor and extracardiac extent. On CMR, hemangiomas are typically heterogeneous with intermediate signal intensity on T1-weighted images and hyperintense on T2-weighted images. They also demonstrate rapid and strong contrast enhancement on first-pass perfusion imaging and typically absent on LGE images, although focal areas of fibrosis may be present [52–54]. On non-contrast CCT, hemangiomas may demonstrate heterogeneous appearance with possible foci of calcification which intensely enhances following contrast administration [47,54].

Malignant cardiac tumors

Cardiac sarcoma

Cardiac sarcomas are the most common primary malignant cardiac tumors (over 95%) [55]. There are many different subtypes of sarcomas, angiosarcoma, and undifferentiated sarcoma being the most common in the heart, often found in the right atrium and in the left atrium, respectively [56]. Angiosarcoma appears lobulated, hyperechogenic, heterogeneous with areas of necrosis or hemorrhage on echocardiography. Despite its vascularity, they do not always enhance with echo contrast [57]. Other sarcomas include leiomyosarcoma and fibrosarcoma, often found in the left atrium, rhabdomyosarcoma in the left ventricle, and synovial sarcoma in the right atrium [31]. On CMR, angiosarcomas show heterogeneous T1- and T2-signal intensity patterns that reflect tumor tissue, necrosis and hemorrhage, early arterial phase enhancement due to vascularity and heterogeneous enhancement pattern on LGE imaging due to peripheral fibrosis and internal hypointensity due to central necrosis. Rhabdomyosarcomas are isointense on T1-weighted images, hyperintense on T2-weighted images, and typically demonstrate homogeneous contrast enhancement with areas of hypointensity due to central necrosis. Undifferentiated sarcomas generally show similar CMR features as that of angiosarcoma [42]. On CCT, angiosarcoma is characterized by broad based attachment with hematogenous connection with the tumor cavity which may be seen on early imaging. Delayed contrast imaging allows for better visualization of the tumor cavity with heterogeneous appearance given scattered areas of non-enhancing necrosis. Invasion to adjacent structures may also be identified. Rhabdomyosarcomas appear as large, infiltrative low attenuation masses that may surround a central area of necrosis. CCT is useful for evaluating extracardiac extension of the tumor as well as distant metastases.

Primary cardiac lymphoma

Cardiac lymphomas are the second most common primary malignant cardiac tumors after sarcomas [55]. On echocardiography, cardiac lymphomas appear lobular or nodular mass with homogeneous echogenicity, or “thickened wall” appearance with restrictive physiology. They are more commonly found in the right chambers, especially the right atrium. On CMR, lymphomas appear homogenous due to lack of central regions of necrosis and hemorrhage. They are isointense to myocardium on T1- and T2- weighted images with slow contrast uptake on LGE images which helps distinguish them from other malignant tumors [32,58]. CMR can further depict the extent of myocardial and pericardial infiltration. On CCT, lymphoma demonstrates iso-hypoattenuation relative to myocardium, extending and infiltrating into the myocardium, pericardium, great vessels and coronary arteries with heterogeneous enhancement after contrast administration [59]. PET/CT has been increasing used for staging and follow-up of lymphomas, especially more aggressive types with high glucose metabolism and SUV numbers [60].

Metastatic cardiac tumors

Secondary cardiac tumors are generally formed by direct extension, hematogenous spread, or lymphatic spread [13], and can be found in around 7% of persons with known malignancies [61]. Due to its hematogenous spread, malignant melanoma has the highest potential for cardiac metastasis [62]. Other common cancers metastasize to the heart are lung, breast, esophageal carcinomas, lymphoma, and leukemia [63•].

Echo remains the first diagnostic test for anyone with suspected cardiac metastasis. CCT also provide detailed evaluation of the adjacent lung and mediastinal structures. Often metastatic disease is already suspected due to a history of a primary malignancy and/or other extracardiac metastases. In this case, the primary role of imaging is to precisely depict the anatomic relationship of the cardiac mass, rather than evaluate its tissue characteristic. In this regard, the high spatial resolution of CT and its ability to image nearby extracardiac structures make it well suited to evaluate and monitor cardiac metastases. CMR remains the best modality for evaluating cardiac involvement of metastasis by identifying direct extension from adjacent extracardiac structures with tissue characterization [63•]. Additionally, hemorrhagic and exudative pericardial effusions, signs of malignant pericardial effusion, demonstrate high signal intensity on T1-weighted images in contrast to low signal intensity demonstrated by benign transudative fluid. Metastases generally demonstrate low signal intensity on T1-weighted images and high signal intensity on T2-weighted images except for melanoma metastases which may appear bright on T1-weighted images due to amount of melanin pigment. Contrast enhancement is usually heterogeneous [42]. ^{18}F-FDG PET imaging demonstrates increased tracer uptake within metastatic lesions and can aid in the detection of additional metastatic lesions as well as the primary neoplasm. Hybrid PET/CT or PET/MRI in addition can be useful for more comprehensive evaluation [63•].

Carcinoid heart disease

Over half of the patients with carcinoid syndrome have cardiac involvement, commonly leading to fibrous deposition of the tricuspid and pulmonic valves, as well as left-sided valves for those with right-to-left shunts. There is rarely tumor infiltration of the endocardium and myocardium [64]. TTE often demonstrates thickened tricuspid and pulmonic valve leaflets, leading to regurgitation and/or stenosis. In rare occasion of tumor metastasis, TTE can identify large tumors. Abnormal right and global left ventricular strain imaging has been shown in patients with carcinoid heart disease [65]. CMR has emerged as the predominant modality to assess cardiac carcinoid, both in the evaluation of valvular disease and myocardial involvement. CCT can demonstrate valvular calcification, chamber size, and coronary involvement [64]. Lastly, nuclear imaging with octreotide SPECT or PET has high sensitivity and specificity for identifying metastatic neuroendocrine tumor with cardiac and other organ involvement [66].

Conclusion

With the advances in cardiac imaging, a multimodality approach is crucial in the evaluation of intracardiac masses. Each imaging modality provides different information regarding the lesion of interest and complements one another with its advantages and disadvantages. Ultimately the choice of imaging modality

should be individualized to provide the diagnosis and management of cardiac masses.

Compliance with Ethical Standards

Conflict of Interest
The authors declare that they have no conflicts of interest.

Human and Animal Rights and Informed Consent
This article does not contain any studies with human or animal subjects performed by any of the authors.

References and Recommended Reading

Papers of particular interest, published recently, have been highlighted as:
- • Of importance
- •• Of major importance

1. Lam KY, Dickens P, Chan ACL. Tumors of the heart: a 20-year experience with a review of 12,485 consecutive autopsies. Arch Pathol Lab Med. 1993;117:1027–31.
2. Pazos-López P, Pozo E, Siqueira ME, García-Lunar I, Cham M, Jacobi A, et al. Value of CMR for the differential diagnosis of cardiac masses. JACC Cardiovasc Imaging. 2014;7:896–905. https://doi.org/10.1016/j.jcmg.2014.05.009.
3. Gupta S, Plein S, Greenwood JP. The Coumadin Ridge: an important example of a left atrial pseudotumour demonstrated by cardiovascular magnetic resonance imaging. J Radiol Case Rep. 2009;3:1–5. https://doi.org/10.3941/jrcr.v3i9.210.
4. Burke A, Tavora F. The 2015 WHO Classification of tumors of the heart and pericardium. J Thorac Oncol. 2016;11:441–52. https://doi.org/10.1016/j.jtho.2015.11.009.
5. Lang RM, Goldstein SA, Kronzon I, Khandheria BK, Mor-Avi V, American Society of Echocardiography. ASE's comprehensive echocardiography 2015.
6. Mügge A, Daniel WG, Haverich A, Lichtlen PR. Diagnosis of noninfective cardiac mass lesions by two-dimensional echocardiography. Comparison of the transthoracic and transesophageal approaches. Circulation. 1991;83:70–8.
7. Reeder GS, Khandheria BK, Seward JB, Tajik AJ. Transesophageal echocardiography and cardiac masses. Mayo Clin Proc. 1991;66:1101–9. https://doi.org/10.1016/S0025-6196(12)65788-7.
8. •• Mankad R, Herrmann J. Cardiac tumors: echo assessment. Echo Res Pract. 2016;3:R65–77. https://doi.org/10.1530/erp-16-0035
Comprehensive echocardiographic evaluation of the most common cardiac masses in detail with algorithms.
9. Kirkpatrick JN, Wong T, Bednarz JE, Spencer KT, Sugeng L, Ward RP, et al. Differential diagnosis of cardiac masses using contrast echocardiographic perfusion imaging. J Am Coll Cardiol. 2004;43:1412–9. https://doi.org/10.1016/J.JACC.2003.09.065.
10. Asch FM, Bieganski SP, Panza JA, Weissman NJ. Real-time 3-dimensional echocardiography evaluation of intracardiac masses. Echocardiography. 2006;23:218–24. https://doi.org/10.1111/j.1540-8175.2006.00196.x.
11. Plana JC. Added value of real-time three-dimensional echocardiography in assessing cardiac masses. Curr Cardiol Rep. 2009;11:205–9. https://doi.org/10.1007/s11886-009-0029-5.
12. Ganame J, D'hooge J, Mertens L. Different deformation patterns in intracardiac tumors. Eur J Echocardiogr. 2005;6:461–4. https://doi.org/10.1016/j.euje.2005.02.006.
13. • Palaskas N, Thompson K, Gladish G, Agha AM, Hassan S, Iliescu C, et al. Evaluation and management of cardiac tumors. Curr Treat Options Cardiovasc Med. 2018;20:29. https://doi.org/10.1007/s11936-018-0625-z
Provides overview of multimodality evaluation and management of common cardiac tumors.
14. Greenwood JP, Motwani M, Crean AM. Cardiac tumours. Adv Card Imaging. 2015:585–616. https://doi.org/10.1016/B978-1-78,242-282-2.00017-2.
15. Finn JP, Nael K, Deshpande V, Ratib O, Laub G. Cardiac MR imaging: state of the technology. Radiology. 2006;241:338–54. https://doi.org/10.1148/radiol.2412041866.
16. Altbach MI, Squire SW, Kudithipudi V, Castellano L, Sorrell VL. Cardiac MRI is complementary to

echocardiography in the assessment of cardiac masses. Echocardiography. 2007;24:286–300. https://doi.org/10.1111/j.1540-8175.2007.00392.x.

17. Patel R, Lim RP, Saric M, Nayar A, Babb J, Ettel M, et al. Diagnostic performance of cardiac magnetic resonance imaging and echocardiography in evaluation of cardiac and paracardiac masses. Am J Cardiol. 2016;117:135–40. https://doi.org/10.1016/j.amjcard.2015.10.014.
18. Mousavi N, Cheezum MK, Aghayev A, Padera R, Vita T, Steigner M, et al. Assessment of cardiac masses by cardiac magnetic resonance imaging: histological correlation and clinical outcomes. J Am Heart Assoc 2019;8. doi:https://doi.org/10.1161/JAHA.117.007829.
19.•• Doherty JU, Kort S, Mehran R, Schoenhagen P, Soman P, Dehmer GJ, et al. ACC/AATS/AHA/ASE/ASNC/HRS/SCAI/SCCT/SCMR/STS 2019 Appropriate use criteria for multimodality imaging in the assessment of cardiac structure and function in nonvalvular heart disease. J Am Coll Cardiol. 2019;73:488–516. https://doi.org/10.1016/j.jacc.2018.10.038

Appropriate use criteria for multimodality imaging, statement from major cardiology societies.

20. Taylor AJ, Cerqueira M, Hodgson JMB, Mark D, Min J, O'Gara P, et al. ACCF/SCCT/ACR/AHA/ASE/ASNC/NASCI/SCAI/SCMR 2010 Appropriate use criteria for cardiac computed tomography. J Cardiovasc Comput Tomogr. 2010;4:407.e1–407.e33. https://doi.org/10.1016/j.jcct.2010.11.001.
21. Hong YJ, Hur J, Han K, Im DJ, Suh YJ, Lee HJ, et al. Quantitative analysis of a whole cardiac mass using dual-energy computed tomography: comparison with conventional computed tomography and magnetic resonance imaging. Sci Rep. 2018;8:15334. https://doi.org/10.1038/s41598-018-33,635-0.
22. Hong YJ, Hur J, Kim YJ, Lee HJ, Hong SR, Suh YJ, et al. Dual-energy cardiac computed tomography for differentiating cardiac myxoma from thrombus. Int J Card Imaging. 2014;30:121–8. https://doi.org/10.1007/s10554-014-0490-0.
23. Saponara M, Ambrosini V, Nannini M, Gatto L, Astolfi A, Urbini M, et al. 18F-FDG-PET/CT imaging in cardiac tumors: illustrative clinical cases and review of the literature. Ther Adv Med Oncol. 2018;10:1–9. https://doi.org/10.1177/1758835918793569.
24. Rahbar K, Seifarth H, Schafers M, Stegger L, Hoffmeier A, Spieker T, et al. Differentiation of malignant and benign cardiac tumors using 18F-FDG PET/CT. J Nucl Med. 2012;53:856–63. https://doi.org/10.2967/jnumed.111.095364.
25. Nensa F, Tezgah E, Poeppel TD, Jensen CJ, Schelhorn J, Kohler J, et al. Integrated 18F-FDG PET/MR imaging in the assessment of cardiac masses: a pilot study. J Nucl Med. 2015;56:255–60. https://doi.org/10.2967/jnumed.114.147744.
26. Kuester LB, Fischman AJ, Fan CM, Halpern EF, Aquino SL. Lipomatous hypertrophy of the interatrial septum: prevalence and features on fusion 18F fluorodeoxyglucose positron emission tomography/CT. Chest. 2005;128:3888–93. https://doi.org/10.1378/chest.128.6.3888.
27. Wibmer AG, Hricak H, Ulaner GA, Weber W. Trends in oncologic hybrid imaging. Eur J Hybrid Imaging. 2018;2:1. https://doi.org/10.1186/s41824-017-0019-6.
28. Krumm P, Mangold S, Gatidis S, Nikolaou K, Nensa F, Bamberg F, et al. Clinical use of cardiac PET/MRI: current state-of-the-art and potential future applications. Jpn J Radiol. 2018;36:313–23. https://doi.org/10.1007/s11604-018-0727-2.
29. Feinberg DA, Giese D, Bongers DA, Ramanna S, Zaitsev M, Markl M, et al. Hybrid ultrasound MRI for improved cardiac imaging and real-time respiration control. Magn Reson Med. 2010;63:290–6. https://doi.org/10.1002/mrm.22250.
30. Nensa F, Bamberg F, Rischpler C, Menezes L, Poeppel TD, la Fougère C, et al. Hybrid cardiac imaging using PET/MRI: a joint position statement by the European Society of Cardiovascular Radiology (ESCR) and the European Association of Nuclear Medicine (EANM). Eur Radiol. 2018;28:4086–101. https://doi.org/10.1007/s00330-017-5008-4.
31. Abels B, Pfeiffer S, Stix J, Schwab J. Multimodal imaging for the assessment of a cardiac mass—a case of primary cardiac sarcoma. J Radiol Case Rep. 2017;11:11–9. https://doi.org/10.3941/jrcr.v11i11.3194.
32. O'Donnell DH, Abbara S, Chaithiraphan V, Yared K, Killeen RP, Cury RC, et al. Cardiac tumors: optimal cardiac MR sequences and spectrum of imaging appearances. Am J Roentgenol. 2009;193:377–87. https://doi.org/10.2214/AJR.08.1895.
33. Barkhausen J, Hunold P, Eggebrecht H, Schüler WO, Sabin GV, Erbel R, et al. Detection and characterization of intracardiac thrombi on MR imaging. Am J Roentgenol. 2002;179:1539–44. https://doi.org/10.2214/ajr.179.6.1791539.
34. Hur J, Pak HN, Kim YJ, Lee HJ, Chang HJ, Hong YJ, et al. Dual-enhancement cardiac computed tomography for assessing left atrial thrombus and pulmonary veins before radiofrequency catheter ablation for atrial fibrillation. Am J Cardiol. 2013;112:238–44. https://doi.org/10.1016/j.amjcard.2013.03.018.
35. Możeńska O, Sypuła S, Celińska-Spoder M, Walecki J, Kosior DA. Mitral annulus caseous calcification mimicking cardiac mass in asymptomatic patient—multimodality imaging approach to incidental echocardiographic finding. Pol J Radiol. 2014;79:88–90. https://doi.org/10.12659/PJR.889830.
36. Colin GC, Gerber BL, Amzulescu M, Bogaert J. Cardiac myxoma: a contemporary multimodality imaging review. Int J Card Imaging. 2018;34:1789–808. https://doi.org/10.1007/s10554-018-1396-z.
37. Burke AP, Virmani R. Cardiac myxoma. A clinicopathologic study. Am J Clin Pathol. 1993;100:671–80. https://doi.org/10.1093/ajcp/100.6.671.
38. Goldberg HP, Glenn F, Dotter CT, Steinberg I. Myxoma of the left atrium; diagnosis made during life with

operative and post-mortem findings. Circulation. 1952;6:762–7.
39. Handke M, Goepfrich M, Keller H. Strongly neovascularized left atrial myxoma. Eur J Echocardiogr. 2008;9:99–100. https://doi.org/10.1016/j.euje.2007.03.039.
40. Engberding R, Daniel WG, Erbel R, Kasper W, Lestuzzi C, Curtius JM, et al. Diagnosis of heart tumours by transoesophageal echocardiography: a multicentre study in 154 patients. Eur Heart J. 1993;14:1223–8. https://doi.org/10.1093/eurheartj/14.9.1223.
41. Abbas A, Garfath-Cox KAG, Brown IW, Shambrook JS, Peebles CR, Harden SP. Cardiac MR assessment of cardiac myxomas. Br J Radiol. 2015;88:20140599. https://doi.org/10.1259/bjr.20140599.
42. Motwani M, Chb MB, Kidambi A, Bch BM, Herzog BA, Uddin A, et al. MR imaging of cardiac tumors and masses: a review of methods and clinical applications 2013;268:26–43.
43. Gheysens O, Cornillie J, Voigt JU, Bogaert J, Westhovens R. Left atrial myxoma on FDG-PET/CT. Clin Nucl Med. 2013;38:e421–2. https://doi.org/10.1097/RLU.0b013e31827086a3.
44. McAllister HA, Hall RJ, Cooley DA. Tumors of the heart and pericardium. Curr Probl Cardiol. 1999;24:59–116. https://doi.org/10.1016/S0146-2806(99)80001-2.
45. Gowda RM, Khan IA, Nair CK, Mehta NJ, Vasavada BC, Sacchi TJ. Cardiac papillary fibroelastoma: a comprehensive analysis of 725 cases. Am Heart J. 2003;146:404–10. https://doi.org/10.1016/S0002-8703(03)00249-7.
46. Bass JL, Breningstall GN, Swaiman KF. Echocardiographic incidence of cardiac rhabdomyoma in tuberous sclerosis. Am J Cardiol. 1985;55:1379–82. https://doi.org/10.1016/0002-9149(85)90508-9.
47. Grebenc ML, Rosado de Christenson ML, Burke AP, Green CE, Galvin JR. Primary cardiac and pericardial neoplasms: radiologic-pathologic correlation. Radiographics. 2000;20:1073–103. https://doi.org/10.1148/radiographics.20.4.g00jl081073.
48. Buckley O, Madan R, Kwong R, Rybicki FJ, Hunsaker A. Cardiac masses, part 2: key imaging features for diagnosis and surgical planning. Am J Roentgenol. 2011;197:W842–51. https://doi.org/10.2214/ajr.11.6903.
49. Shapiro LM. Cardiac tumours: diagnosis and management. Heart. 2001;85:218–22. https://doi.org/10.1136/heart.85.2.218.
50. Kojima S, Sumiyoshi M, Suwa S, Tamura H, Sasaki A, Kojima T, et al. Cardiac hemangioma: a report of two cases and review of the literature. Heart Vessel. 2003;18:153–6. https://doi.org/10.1007/s00380-003-0699-7.
51. Papadopoulos K, Makrides CA, Eleutheriou E. A cardiac haemangioma: the contribution of myocardial contrast echocardiography in the diagnosis. BMJ Case Rep. 2015;2015:bcr2015210075. https://doi.org/10.1136/bcr-2015-210,075.
52. Kiaffas MG, Powell AJ, Geva T. Magnetic resonance imaging evaluation of cardiac tumor characteristics in infants and children. Am J Cardiol. 2002;89:1229–33. https://doi.org/10.1016/S0002-9149(02)02314-7.
53. Oshima H, Hara M, Kono T, Shibamoto Y, Mishima A, Akita S. Cardiac hemangioma of the left atrial appendage: CT and MR findings. J Thorac Imaging. 2003;18:204–6. https://doi.org/10.1097/00005382-200,307,000-00012.
54. Cresti A, Chiavarelli M, Munezero Butorano MA, Franci L. Multimodality imaging of a silent cardiac hemangioma. J Cardiovasc Echogr. 2015;25:31. https://doi.org/10.4103/2211-4122.158427.
55. Hudzik B, Miszalski-Jamka K, Glowacki J, Lekston A, Gierlotka M, Zembala M, et al. Malignant tumors of the heart. Cancer Epidemiol. 2015;39:665–72. https://doi.org/10.1016/j.canep.2015.07.007.
56. Vander Salm TJ. Unusual primary tumors of the heart. Semin Thorac Cardiovasc Surg. 2000;12:89–100. https://doi.org/10.1053/ct.2000.5080.
57. Kupsky DF, Newman DB, Kumar G, Maleszewski JJ, Edwards WD, Klarich KW. Echocardiographic features of cardiac angiosarcomas: the Mayo Clinic experience (1976–2013). Echocardiography. 2016;33:186–92. https://doi.org/10.1111/echo.13060.
58. Dorsay TA, Ho VB, Rovira MJ, Armstrong MA, Brissette MD. Primary Cardiac lymphoma: CT and MR findings. J Comput Assist Tomogr. 1993;17:978–81.
59. Ciancarella P, Fusco A, Citraro D, Sperandio M, Floris R. Multimodality imaging evaluation of a primary cardiac lymphoma. J Saudi Heart Assoc. 2017;29:128–35. https://doi.org/10.1016/j.jsha.2016.09.001.
60. Jhanwar YS, Straus DJ. The role of PET in lymphoma. J Nucl Med. 2006;47:1326–34.
61. Al-Mamgani A, Baartman L, Baaijens M, De Pree I, Incrocci L, Levendag PC. Cardiac metastases. Int J Clin Oncol. 2008;13:369–72. https://doi.org/10.1007/s10147-007-0749-8.
62. Reynen K, Köckeritz U, Strasser RH. Metastases to the heart. Ann Oncol. 2004;15:375–81. https://doi.org/10.1093/annonc/mdh086.
63.• Lichtenberger JP, Reynolds DA, Keung J, Keung E, Carter BW. Metastasis to the heart: a radiologic approach to diagnosis with pathologic correlation. Am J Roentgenol. 2016;207:764–72. https://doi.org/10.2214/AJR.16.16148
Comprehensive review of metastasis to the heart.
64. Agha AM, Lopez-Mattei J, Donisan T, Balanescu D, Iliescu CA, Banchs J, et al. Multimodality imaging in carcinoid heart disease. Open Heart. 2019;6:e001060. https://doi.org/10.1136/openhrt-2019-001060.
65. Haugaa KH, Bergestuen DS, Sahakyan LG, Skulstad H, Aakhus S, Thiis-Evensen E, et al. Evaluation of right ventricular dysfunction by myocardial strain echocardiography in patients with intestinal carcinoid disease. J Am Soc Echocardiogr. 2011;24:644–50. https://doi.org/10.1016/j.echo.2011.02.009.

66. Gabriel M, Decristoforo C, Kendler D, Dobrozemsky G, Heute D, Uprimny C, et al. 68Ga-DOTA-Tyr3-octreotide PET in neuroendocrine tumors: comparison with somatostatin receptor scintigraphy and CT. J Nucl Med. 2007;48:508–18. https://doi.org/10.2967/jnumed.106.035667.

Publisher's Note